Vol. 03, Iss. 1 (2025) 78-86, DOI: 10.61552/JME.2025.01.005

JME

Journal of Materials and Engineering

www.jme.aspur.rs

Research article

Study on Wear Characteristics of Surfaces Coated with HVOF and Aluminium Alloy Using Multi-Body Dynamics Analysis

R. Suresh[a,*], K.M. Vinay[b], M. Prasanna Kumar[c], H.K. Madhusudan[d]

[a]*Department of Mechanical Engineering, University BDT College of Engineering, Davanagere, Karnataka state, India,*
[b]*Department of Industrial and Production Engineering, University BDT College of Engineering, Davanagere, Karnataka state, India,*
[c]*Department of Mechanical Engineering, VTU-CPGS, Mysore. Karnataka state, India,*
[d]*Department of Mechanical Engineering, KLE Technological university Hubli, Karnataka state, India.*

Keywords:

Wear simulation
Archard
HVOF coating
Comsol

* Corresponding author:

R. Suresh
E-mail: sumohi@gmail.com

Received: 23 April 2024
Revised: 22 May 2024
Accepted: 15 June 2024

A B S T R A C T

The objective of this study was to compare and analyze the wear behaviors of High-Velocity Oxy-Fuel (HVOF) NiCr-B4C sprayed coated Al6061MMC and Al6061 alloy. Surface coatings are widely used for their excellent wear resistance and low friction performance. Wear prediction is crucial for the engineering application of these components. In this work, the wear simulation approach using COMSOL, a commercial finite element (FEA) program, is presented. The findings presented here are based on a stabilized model obtained through several software iterations exploring different options. The wear depth of Al6061 alloy and HVOF Coated Al6061MM is evaluated using the linear Archad's wear law. The pins on disc components are assumed to have 3-dimensional flexible shapes and the contact surfaces exhibit elastic-plastic material behavior. The impact of debris and oxide production pathways is considered by utilizing a wear coefficient (k) derived from experimental investigation. HVOF-sprayed coatings based on Ni80Cr20-B4C have shown promising tribological characteristics for wear applications. The results of the finite element simulation are in good agreement with the experimental result.

1. INTRODUCTION

Wear is a highly intricate phenomenon that can be classified based on its failure mechanism, including adhesive wear, abrasive wear, surface fatigue, and corrosion. Adhesive wear occurs when rough surfaces interact, resulting in the transfer of metal from one surface to another. However, due to the lack of consideration for chemical interactions between bodies or surfaces in finite element programs, these types of wear are not discussed in this paper.

Wear is a highly intricate phenomenon that can be classified based on its failure mechanism, including adhesive wear, abrasive wear, surface fatigue, and corrosion. Adhesive wear occurs when rough surfaces interact, resulting in the transfer of metal from one surface to another. However, due to the lack of consideration for chemical interactions between bodies or surfaces in finite element programs, these types of wear are not discussed in this paper.

There are two possible approaches to carry out finite element modelling of dry sliding wear. The first approach involves incorporating and calculating the details of the surface interaction, such as surface finish, within the model. If this method is chosen, it would necessitate the removal of individual finite elements from the model in order to simulate gouging or plowing. Consequently, the size of the finite element must match the size of the particles being removed, as there are currently no provisions for removing a portion of an element in the simulation software [1].

Extensive research has been conducted in the field of wear modeling to develop predictive governing equations. The literature on wear modeling can be broadly categorized into two main types: mechanistic models and phenomenological models. On the other hand, phenomenological models involve quantities that need to be computed using principles of contact mechanics, such as the Archard-based wear model. These models have been extensively studied by combining them with numerical calculations, such as finite element analysis [2].

2. WEAR SIMULATION METHOD

Archard's law is a commonly employed wear law that establishes a straightforward relationship between the volume of material worn away "W", the normal contact force"F_N", the sliding distance "L_T", the material hardness "H", and a constant "K" specific to the material(equation 1) The wear constant may be computed from experimental wear data, which is typically in the form of weight loss for a specific contact pressure and velocity.

$$W = (K F_N L_T) /H \quad (1)$$

Finite element analysis (FEA) codes do not typically include wear equations, but it is relatively simple to incorporate them into COMSOL Multiphysics. In our simulations, we have integrated the wear equations by defining boundary ordinary differential equations (ODEs) on the contact surfaces where wear occurs. The wear depth serves as the independent variable in these equations. By using the wear depth as an offset between the contacting surfaces, such as a pin and disc, we are able to accurately model the contact formulation in COMSOL Multi physics [3].

2.1 Multibody dynamics

Wear simulation requires the discretization of a continuous process into many phases. Assume that the contact parameters—such as surface shape and contact pressure—remain constant at each stage. The initial step in the wear simulation process is determining the contact pressure between the contact surfaces. Since contact problems are typically non-linear, contact parameters are determined using the commercial finite element program Comsol 5.0.Because it does not require changing the nodal locations to account for material loss due to wear, this wear algorithm is incredibly efficient. However, it is only appropriate in situations when the wear depth is much smaller than the contact surface's width. More complex effects, such as anisotropic wear behaviour, dependency on the solid's mean and deviatoric stresses (rather than just the contact pressure), threshold pressure/stress below which wear doesn't occur, and more, can be included to improve this wear algorithm. To be correct, this modeling approach still relies on the assumption of little wear depth

The pin on disc tribometer set up can be translated in to a FEA model is as shown in figure 1. The pin in this particular model is significantly rigid as compared to the disc, leading to the assumption that all the wear takes place in the disc. When a force is exerted on the pin, it creates a circular contact pressure distribution similar to the Hertzian model. Following this, a constant tangential velocity is imparted to the disc.

A prevalent approach to calculate the value of K involves applying a preload of P to a stationary pin, which is then pressed into the surface of a rotating disk. The load P is already known, and the sliding distance L_T can be determined by analyzing the rotational speed and duration of the disk's rotation.

The wear on the pin is assessed by measuring the change in mass (weight) of the pin and calculating the constant K. However, this method has its limitations when it comes to determining a constant wear coefficient for a specific pair of surfaces.

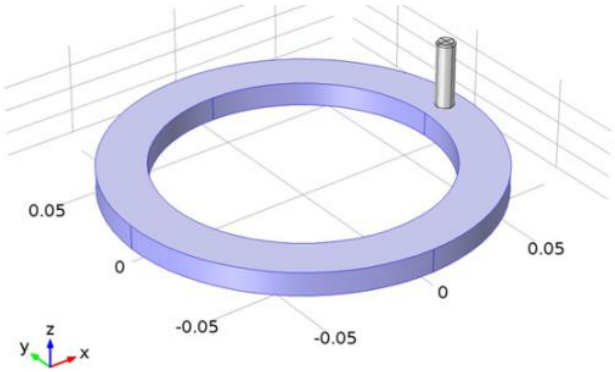

Fig. 1. Pin-on-disc FEA simulation model.

It fails to account for changes in the apparent area of contact over time, which is commonly referred to as "running in" effects. Despite the limitations mentioned, it is important to note that the assumption of a constant load direction may not always hold true in real-world scenarios. Additionally, the assumption that the surface topography of experimental surfaces accurately represents the surfaces of interest may also be subject to discrepancies. However, despite these potential limitations, it is still deemed acceptable to assume that the wear coefficients obtained through the pin-on-disk method or other methods are sufficiently accurate for use in engineering analysis [4]. The wear depth of the given contact geometry with given loading will not change, if the product K*LT is not changed, regardless of the values of K and L_T.

3. EXPERIMENTAL METHOD

Dry Slide pin-on-disc experiments set up is as shown in figure 2 and were carried out in accordance with the ASTM G99 standard. The experiments focused on the Al6061 alloy, which has a surface hardness of 53HV. The pins used in the experiments were coated with HVOF-coated Al6061 MMC, which was fabricated using the stir casting method. The composition of the coated pins included 2wt% Graphite and 8wt% Al_2O_3. The contact surface of the coated pins was spray-coated with $Ni_{80}Cr_{20}$ (85%$Ni_{80}Cr_{20}$+15% B_4C), which had a surface hardness of 322HV. The disc used in the experiments was made of steel with a hardness of 698 HV. Prior to each test, the samples were thoroughly cleaned with acetone in an ultrasound bath for 10 minutes to remove any residue from the manufacturing process. After cleaning, the samples were dried using a flow of hot air for two minutes, followed by a flow of cold air for another two minutes.

The reduced modulus of contact between two materials is a function of the Young's moduli of material Al6061, Al_2O_3, graphite, NiCr and Boron carbide materials. Mechanical Properties of material both materials pin and disc are listed in table 1.

Table 1. Mechanical properties of material.

Al6061Alloy					
Part	Material	Young's Modulus GPa	Poisson's Ratio	Density Kg/m³	Hardness (HV)
Pin	Al 60601	86.3	0.29	2796	53
Disc	Steel	200	0.3	7850	430
HVOF Coated Al6061 MMC					
Pin	$Ni_{80}Cr_{20}B_4C$	363	0.294	2847	322
Disc	Steel	200	0.3	7850	430

During the conducted experiment, the disc underwent a continuous rotation at a fixed speed of 600 rpm. The disc was subjected to varying loads of 10, 30, and 50N, while maintaining a constant sliding speed and time duration. The sliding distance covered during the experiment was 2000m, with a consistent sliding velocity of 3.76 m/s in table 2 however, it

is important to note that the FEA simulation results presented solely pertain to the 50N load condition. The testing procedure was conducted under average room temperature conditions of 25 ◦ C and approximately 50% relative humidity.

Fig. 2. Dry slide pin-on-disc Tribometer.

Table 2. Experimental parameter.

Load (N)	Speed (m/sec)	Distance (m)	Time (min)	Velocity (rpm)	Track Radius (mm)
50	3.76	2000	9.26	600	70

4. MICROSTRUCTURE STUDIES

The Figure 3, SEM micrographs captured at IIT Bombay of the Aluminium alloy 6061/Gr(2%)/ Al_2O_3 (8%) fabricated through stir casting exhibit a consistent distribution of Al_2O_3 and graphite particulates throughout the matrix alloy, as depicted in figure 3. Furthermore, there is a strong interface bonding between the reinforcements and the base metal. It has been documented that MMCs with lower porosity tend to possess higher hardness. The investigation into the tribological behaviour and its correlation with the processing and microstructures of Al6061 Metal Matrix Composites reveals that the matrix and reinforcement particulates are well-bonded, resulting in efficient load transfer from the matrix to the reinforcement materials. In the cast Aluminium composite 6061 -8% Al_2O_3, the SEM micrographs also indicate the presence of particle clustering and agglomerations of porosity. Similar findings were also observed by G. B. Veeresh Kumar et al .

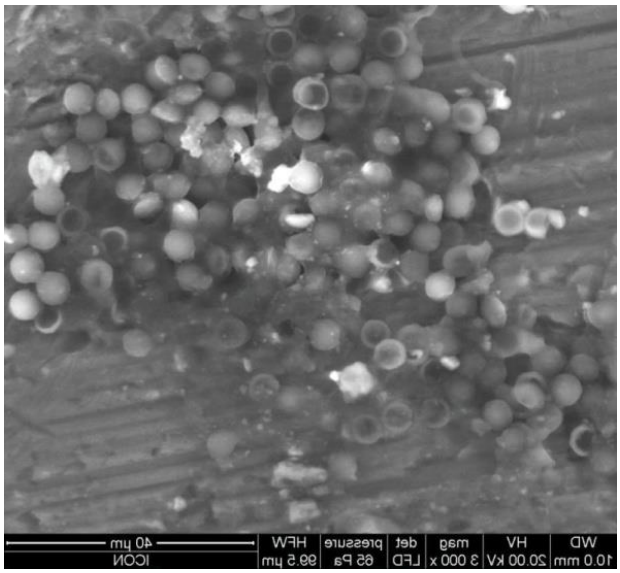

Fig. 3. Microstructure Showing Good Interfacial Bonding between Al6061-Gr- Al_2O_3.

Figure 4 displays the surface SEM micrograph ofthe HVOF method, showcasing the even dispersion of Boron carbide particles within the Nickle chromium matrix. This matrix has undergone ball milling for a duration of 12-15 hours. The analysis of all the coatings indicates a strong bond between the metal matrix and the reinforcement. The microstructure examination reveals that both Nickle Chromium and Boron Carbide are uniformly coated with a thickness ranging from 180 to 200µm on the surface of Al 60601 MMC. These observations are in line with the researcher TaharSahraou et al.

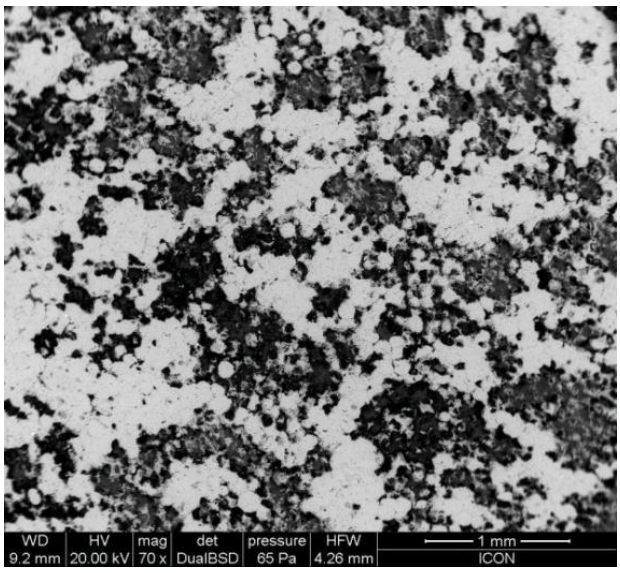

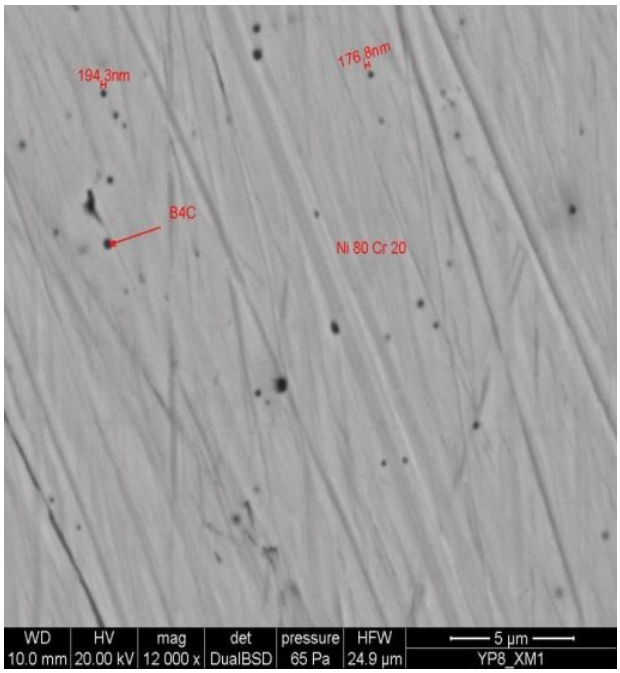

Fig. 4. Uniform reinforcement of B4C & Ni80Cr20 particles in coating.

5. WEAR DEPTH SIMULATION

5.1 Boundary conditions for FE model

The pin exerts a specific load on the disk by placing its end in direct contact with the disk, perpendicular to its surface. According to the ASTMG99 standard, the disk rotates around its center. In certain cases, wear is measured by the volumetric losses in relation to the sliding distance.The pin is considered to be rigid, while the surface of the disc is considered to be flexible and capable of rotation as shown in figure 5. The surface elements of the pin are treated as rigid target elements, while the bottom surface elements of the steel disc are treated as flexible contact elements. The wear calculations are performed using the output obtained from the Finite Element Analysis (FEA) in the previous iteration, which takes into account the contact pressure and sliding distance. These calculations are applicable to all load conditions, including normal loads of 10, 30, and 50 N applied to the top face of the pin. The displacement in the x and y directions at the pin is constrained, allowing only angular rotation of the pin around the disc, resulting in the formation of a wear track.

In order to calculate the wear depth based on contact pressure as the contact surface area varies over time and its sliding distance, FEA dry slide simulation was used. The study of transient non-linear analysis is the main focus of current research in order to capture the non-linear behavior interaction of Pin and Disc in transient load.

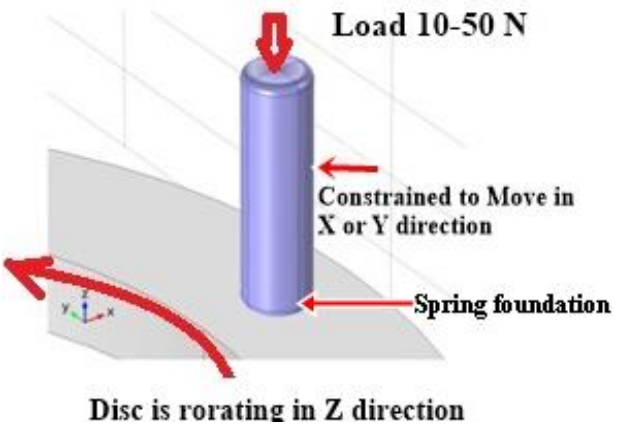

Fig. 5. Boundary conditions.

A weak spring that restricts bodily motion is added to the spring node, and its stiffness is defined by that spring [5,6,7].

5.2 Mesh consistency

In mechanical contact modeling, meshing is as important as in any physics and interface. Disc come into contact with the pin is a mesh size “jump”. By this they mean, first that the the finest mesh will be defined Contact Pair as Destination, in turn, the softest material. Source is non-deformable any mesh it describes. Finite Element Analysis model is optimized by means of controlling total number of nodal degrees of freedom. Using the COMSOL Multiphysics program, We have selected four meshes with triangle elements for our numerical simulation Coarse tetrahedral elements, Normal triangular elements Fine edge elements, and finer vortex mesh elements as listed in table 3.

Wear calculations are done on smooth transition of contact and target elements which are tetrahedral, triangular and edge elements Smooth transition helps to get actual results without any distortion. In region of non-interest, coarse mesh has been used, whereas region of interest is meshed with finer elements as we can see in Figure 6. The mesh sensitivity is performed to verify the results variation with element size [3].

Table 3. Types of meshing elements.

Statistics	
Complete mesh	
Element type:	All elements
Tetrahedral elements:	44799
Triangular elements:	10344
Edge elements:	918
Vertex elements:	34
Domain element statistics	
Number of elements:	44799
Minimum element quality:	0.1554
Average element quality:	0.71
Element volume ratio:	2.287E-4
Mesh volume:	8.939E-5 m^3
Maximum growth rate:	3.728
Average growth rate:	1.852

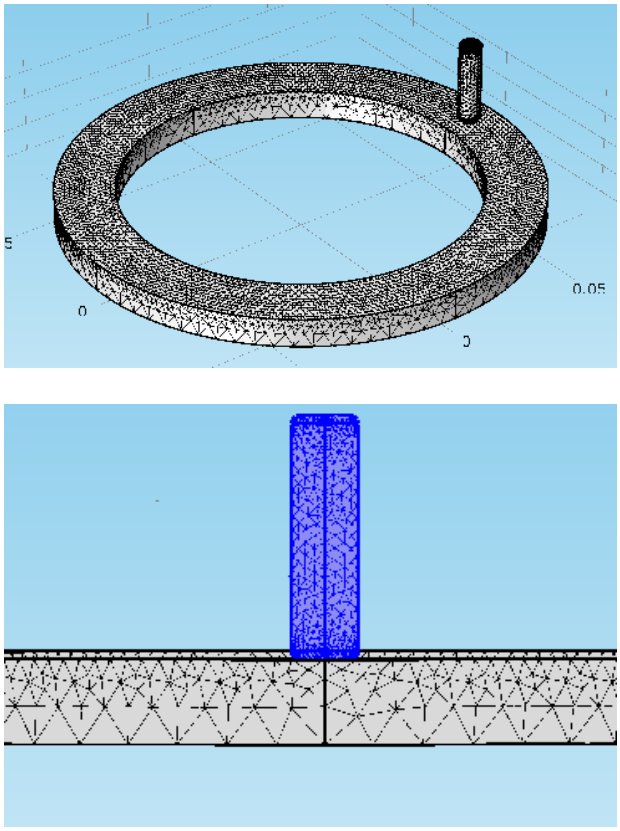

Fig. 6. Meshing of Pin on disc in contact.

6. RESULTS AND DISCUSSION

6.1 Effect of applied load on wear rate

The wear rate of alloy and composites is significantly influenced by the applied load, which is the primary factor controlling wear behavior. When the load is increased at a constant speed, the wear rate of Al 6061 composites and the matrix also increases. This phenomenon was also observed in a study by. Examination of SEM micrographs (figure 7) revealed that at a load of 50N, the exposed Al_2O_3 particles become fractured and become trapped between the steel counterface and the Al 6061 matrix. The fractured Al_2O_3 particles, along with sharp asperities on the counterface, easily penetrate the graphite film, resulting in the formation of coarser and deeper grooves and an increase in wear rate. Similar results were reported by Veeresh Kumar et al. The intense wear was characterized by extensive surface damage and significant aluminum transfer to the opposing surface, along with the production of large debris particles, usually in plate-like shapes with a glossy metallic look. These characteristics were easily noticeable during the test without the aid of any magnifying tools.

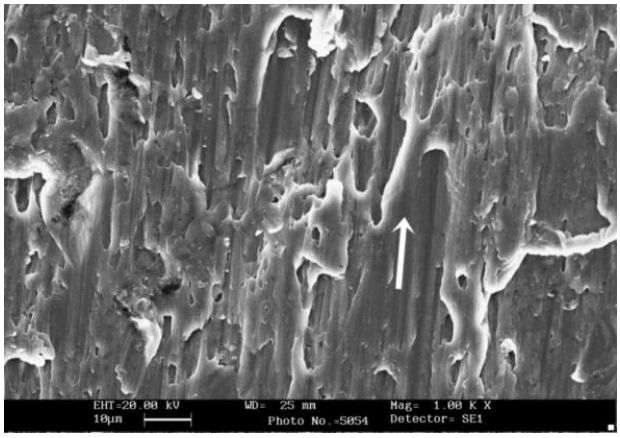

Fig. 7. SEM Micrograph of the worn surface with load 50N.

Results showed that the weight loss during the wear test was highest when using a load of 50N and lowest with a load of 10N. This indicates that as the load increases, the wear rate also increases, as shown in figure 8. Analysis of the worn surface topographies revealed that the dominant Nickel chromium Phase containing B4C particles are securely embedded in the matrix, preventing the soft matrix from being removed by micro-cutting mechanisms, a phenomenon observed in other composite materials. It is evident that the Ni80C20r-B4C particles effectively shield the coated surface, limiting material removal by the counterpart show some porosity in the coated surface. Similar findings were reported by C.-J. Li et al. in their research.

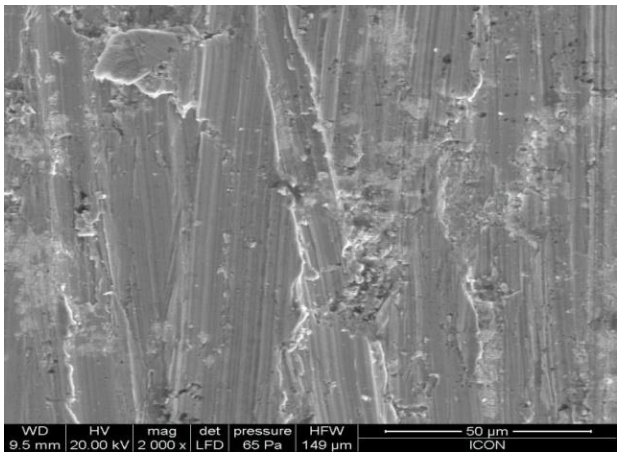

Fig. 8. Worn surface & sliding direction of wear with increase in load 50N.

6.2 Contact analysis

Contact pressure magnitudes have been determined in a stationary investigation for various loading magnitudes of 10, 20, 30, 40, and 50 N. P is the contact pressure, and V is the point under consideration's sliding velocity. It has been assumed that the size of the contact pressure cannot be changed by the wear rate alone. The simulation maintains a constant rotation speed of the disc, which is in frictional contact with the pin upon application of contact pressure as seen if fig. Contact pressure initially concentrated at the leading edge of the pin. Contact pressure gradually spreads out over wider area due as the load goes on increasing to 50N is as shown in fig. 9 and fig. 10. Similar trend is observed from the researchers [3,6].

Contact pressure initially concentrated at the leading edge of the disc contact point of pin (due to friction). Contact pressure gradually spreads out over wider area as load increases. Figure 11 illustrates the comparison between the experimental findings and the FEA simulation for Al606 alloy and HVOF Coated Al6061 MMC [8].

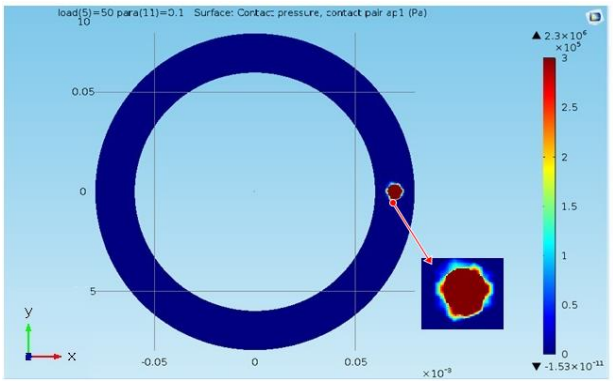

Fig. 9. Al6061 alloy at 50N under contact pressure.

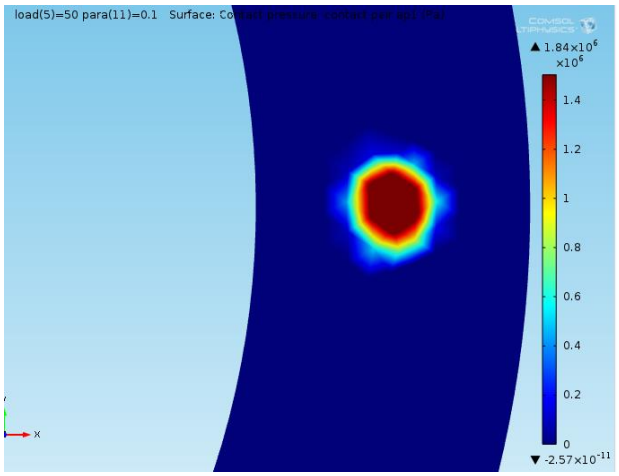

Fig. 10. The contact pressure of Al6061 MMC coated with HVOF at 50N.

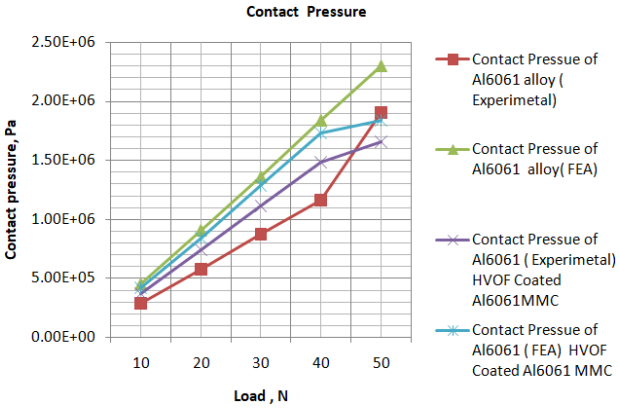

Fig. 11. The contact pressure of Al6061alloy and Al6061 MMC Coated with HVOF

As the load increases the von Mises stress also increases. It clear from the fig. 12 that the Aluminium alloy 6061 experiencing more than the HVOF coated sample [8].

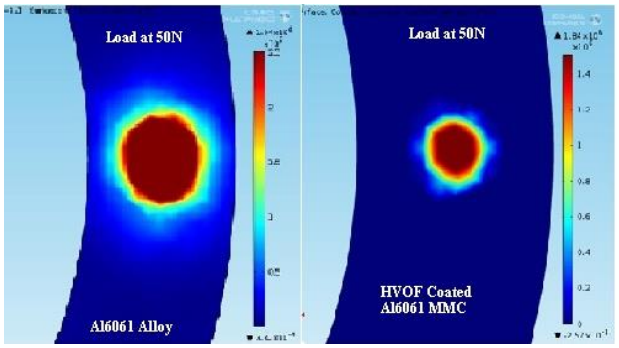

Fig. 12. The von Mises stress of Al6061alloy and Al6061 MM Coated with HVOF at 50N.

The graphical representation in Figure 13 showcases the comparison between the experimental findings and the FEA simulation carried out for Al606 alloy and HVOF Coated Al6061 MMC [8].

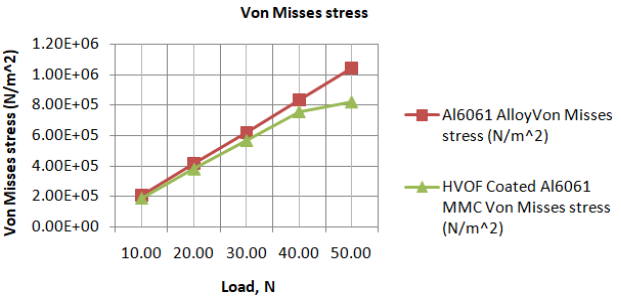

Fig. 13. The von Mises stress of Al6061alloy and Al6061 MMC Coated with HVOF.

6.3 Wear depth

The actual contact area varies depending on the ratio between the pin's angular velocity and the disc's angular velocity [9] The simulation is done only for 2 revolutions and can be extended as many cycles as possible. Wear profile at the end of two cycles, 600 rpm. Refining the mesh will give a smoother wear profile Figure 14 ,15 and Figure 16 depict the wear developed during the FEA simulation for Al6061 alloy and HVOF NiCr-B_4C spray coated surface.

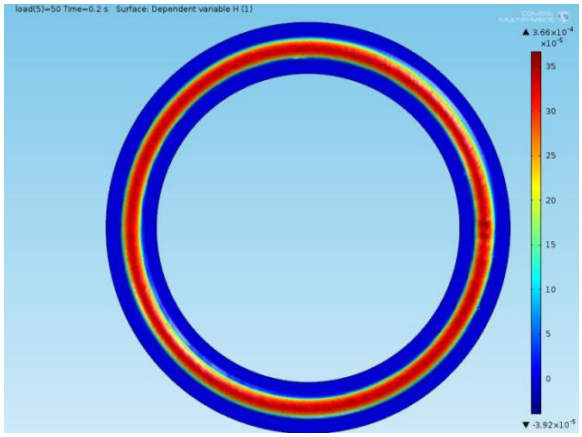

Fig. 14. Al6061 alloy wear contour at 50N.

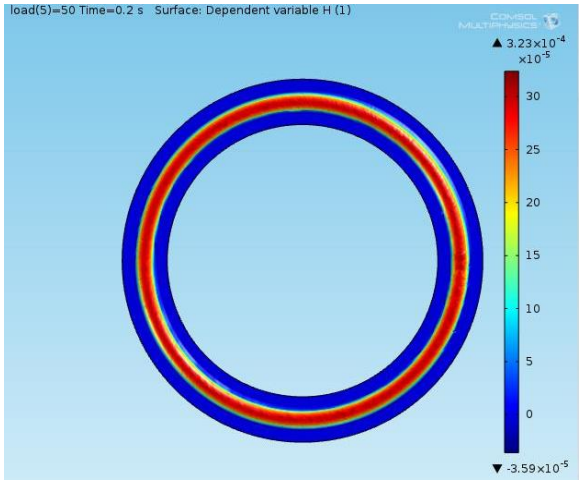

Fig. 15. Al6061 MMC Coated with HVOF wear contour at 50N.

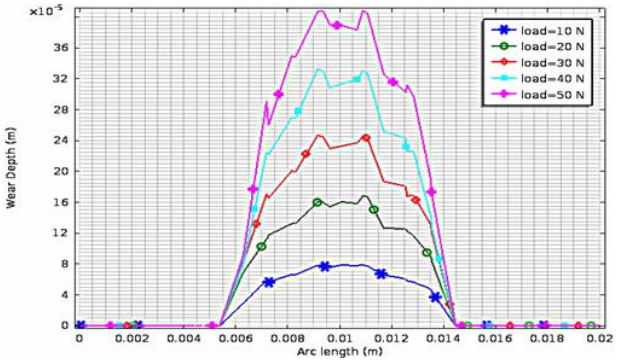

Fig. 16. Wear profile for different loads at 600 rpm.

It was observed that the wear increased with the load, with the minimum and maximum wear occurring at the edge of pin Similar results were found in our earlier work [3,9]. Wear decreases maximum contact pressure and increases contact as shown in fig 17. Wear model failing at 200 sec.

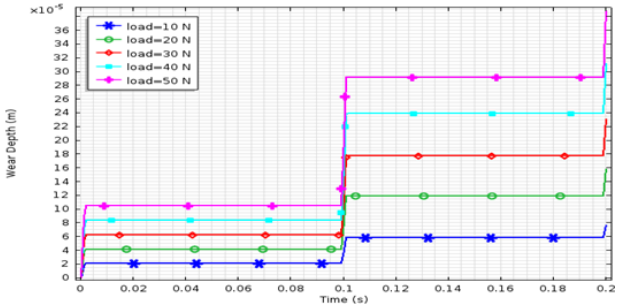

Fig. 17. Wear depth for different loads at 600 rpm.

Total wear volume (integration of wear depth over pin surface) in agreement with theoretical prediction Wear higher at outer radius of pin due to higher sliding velocity.

The wear progression varies across the lining surface due to the uneven distribution of initial contact pressure and sliding velocity. At the beginning, intense stresses occur at the forefront of the pin as a result of friction. As time progresses to 100 seconds, the contact pressure profile becomes more even due to wear. Additionally, we will demonstrate the changes in wear thickness and contact pressure profiles for different cases that involve thermal effects [7].

Notably, the wear was found to be higher in the Al6061 alloy compared to the HVOF coated surface. The average wear values, as shown in Table 4, were used to calculate the FEA wear volume and compared with the experimental wear volume. The results indicate that the

experimental and FEA wear volumes are in better agreement, as depicted in Figure 18. The analysis clearly indicates that an increase in contact pressure at the contour will result in a proportional rise in wear. Renjish Vijay et al also find similar findings. Wear decreases maximum contact pressure and increases contact area can be noticed in fig. Developed a wear model in COMSOL – Boundary ODE representing wear rate equation – Wear depth modifies contact gap condition [8].

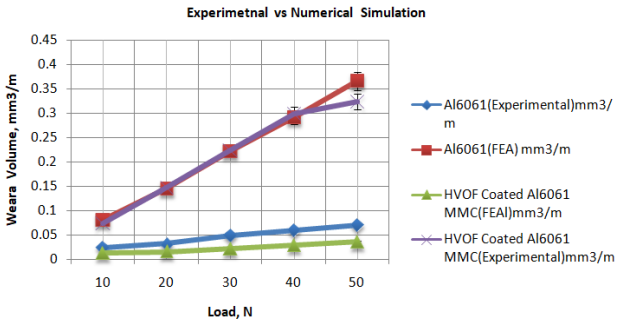

Fig. 18. The contact pressure of Al6061alloy and Al6061 MMC Coated with HVOF.

Tabe 4. Disparity observed between experimental results and finite element analysis outcomes.

Applied Load 50 N	Al6061 MMC (Experimental)	Al6061 MMC (FEA)	% of deviation	HVOF Coated Al6061 MMC (Experimental)	HVOF Coated Al6061 MMC (FEA)	% of deviation
Wear Depth (mm)	0.475	0.363	23.57	0.428	0.323	24.53

7. CONCLUSION

1. The analysis of wear characteristics for Al6061 alloy and HVOF coated Al6061 MMC has been conducted utilizing Archard wear theory and Finite Elemental Analysis. Through this study, the observed phenomena of sliding, contact pressure, and wear depth during the pin on disc experiment have been effectively explained.
2. The contact pressure in the central region of the contact area has been identified as high, potentially resulting in localized wear. The area with the highest contact pressure exhibited the most significant wear, while the opposite was observed in the region with the lowest contact pressure. Finer meshing can enhance the accuracy of the results, although it may come at the cost of increased time needed to obtain the solution.
3. Coated specimen's shows high wear resistance property than the uncoated specimens.
4. Total wear volume (integration of wear depth over pin surface) in agreement with theoretical prediction
5. Wear decreases maximum contact pressure and increases contact area
6. Wear initially concentrated at the leading edge of the pin and gradually spreads out over wider area due to higher sliding velocity.

REFERENCES

[1] L. J. Yang, "Wear coefficient equation for aluminium-based matrix composites against steel disc," *Wear*, vol. 255, pp. 579–592, 2003.

[2] L. Labey, A. Kamali, W. Pascale, and S. Pianigiani, "Development and validation of a Wear Model to Predict Polyethylene Wear in a Total Knee Arthroplasty: A Finite Element analysis," *Lubricants*, B. Innocenti, Ed., vol. 5, no. 2, 2017.

[3] R. Suresh, M. Prasannakumar, S. Basavarajappa, T. S. Kiran, M. Yeole, and N. Katare, "Numerical Simulation & Experimental study of wear depth and contact pressure," *Materials Today: Proceedings*, vol. 4, pp. 11218–11228, 2017.

[4] COMSOL, "Multibody Dynamics User Guide."

[5] V. Hegadekatte, N. Huber, and O. Kraft, "A finite element based technique for simulating sliding wear," presented at the *World Tribology Congress*.

[6] N. Elabbasi, "Simulating Wear in COMSOL Multiphysics," *COMSOL Blog*.

[7] M. B. Serrano Castillo, "Tribology test modeling to obtain the properties of material wear for subsequent optimization."

[8] R. Suresh, M. Prasanna Kumar, and T. S. Kiran, "The Wear Resistance of HVOF Sprayed Nickel Chromium and Boron Carbide Coatings," *International Journal of Engineering Technology Science and Research (IJETSR)*,vol.4, no.5, May 2017.

[9] R. Vijay, V. N. Aju Kumar, A. Sadiq, and R. Rakesh Pillai, "Numerical Analysis of Wear Characteristics of Zirconia Coated Aluminum 6061 Alloy," *IOP Conf. Series: Materials Science and Engineering*, vol. 1059, p. 012020, 2021.